Mechanism of C-3 Hydrogen Exchange and the Elimination of Ammonia in the 3-Methylaspartate Ammonia-Lyase Reaction†

Nigel P. Botting and David Gani*

Department of Chemistry, The Purdie Building, University of St. Andrews, St. Andrews, Fife KY16 9ST, U.K.

Received March 13, 1991; Revised Manuscript Received October 29, 1991

ABSTRACT: The enzyme 3-methylaspartate ammonia-lyase (EC 4.3.1.2) catalyzes the exchange of the C-3 hydrogen of the substrate, (2*S*,3*S*)-3-methylaspartic acid, with solvent hydrogen. The mechanism of the exchange reaction was probed using (2*S*,3*S*)-3-methylaspartic acid and its C-3-deuteriated isotopomer. Incubations conducted in tritiated water allowed the rate of protium or deuterium wash-out from the substrates to be measured as tritium wash-in. The primary deuterium isotope effects for the exchange under essentially V_{max} conditions ([S] $\gg K_m$) were 1.6, 1.5, and 1.5 at pH 9.0, 7.6, and 6.5. The deamination reaction, measured spectrophotometrically on the same incubations, showed isotope effects of 1.7, 1.6, and 1.4 at pH 9.0, 7.6, and 6.5, in agreement with the values of ^{D}V and $^{D}(V/K)$ reported previously [Botting, N. P., Akhtar, M., Cohen, M. A., & Gani, D. (1988) *Biochemistry 27*, 2956–2959]. The ratio of the rate of exchange to the rate of deamination, however, varied widely with pH. Together with the identical values of the primary isotope effects for the two reactions, this result indicates that the partition between reaction pathways occurs after the slowest steps in the common part of the reaction coordinate pathway, almost certainly after the cleavage of the C–N bond at the level of the enzyme–ammonia–mesaconic acid complex, and not at the putative carbanion level as was previously suggested. The enzyme requires both K^+ and Mg^{2+} ions for activity, although ammonium ion is also able to bind in the K^+ site and act as an activator. Variation of the metal ion concentration alters the magnitude of the primary deuterium isotope effects. The variation of potassium ion concentration causes the most marked changes: at 1.6 mM K^+, ^{D}V and $^{D}(V/K)$ are 1.7, whereas at 50 mM K^+, ^{D}V and $^{D}(V/K)$ are reduced to 1.0. The isotope effects are also reduced at low K^+ concentration due to the emergence of a slow-acting high K^+ affinity monopotassium form of the enzyme. The binding order and role of the metal ion cofactors and their influence in determining the formal mechanism of the reaction is discussed, and the failure of previous workers to observe primary deuterium isotope effects for the deamination process is explained. The product desorption order was tested by product inhibition, alternative product inhibition, and isotope exchange experiments. Ammonia and mesaconic acid debind in a random fashion. The enzyme appears to be able to bind ammonium ion in a third mode, in addition to as an activator and as a product. The effect of the occupation of this third site on the deamination process is discussed.

The enzyme 3-methylaspartase (3-methylaspartate ammonia-lyase, EC 4.3.1.2) catalyzes the reversible α,β-elimination of ammonia from L-*threo*-(2*S*,3*S*)-3-methylaspartic acid (**1**) to give mesaconic acid (Scheme I) (Barker et al., 1959). The enzyme lies on the main catabolic pathway for glutamate in *Clostridium tetanomorphum* (Barker et al., 1959) and a number of other species (Williams & Traynham, 1962; Ueda et al., 1982). The clostridial enzyme, which is the best studied, has been shown to deaminate the L-*erythro* 2*S*,3*R* diastereomer of methylaspartic acid (Barker et al., 1959) as well as (2*S*)-aspartic acid and a number of 3-alkyl homologues (Winkler & Williams, 1967). The enzyme, M_r 100 000, was reported to possess an $(AB)_2$ structure (Hsiang & Bright, 1967; Wu & Williams, 1968) and was demonstrated to require both monovalent and divalent cations for activity. The enzyme was shown to catalyze the exchange of the C-3 hydrogen atom of the physiological substrate with hydrogen derived from the solvent, at greater rates than the overall deamination under some conditions. No primary deuterium isotope effect was detected for the deamination reaction over the pH range 5.5–10.5. The pH optimum for V_{max} is 9.7. On the basis of these observations together with the reported ability of the enzyme to process both diastereomers of L-3-methylaspartic acid, a mechanism involving the intermediacy of a carbanion was proposed (Bright, 1964; Bright et al., 1964a) [see Hansen and Havir (1970) for a review of the early work]. Since Bright's work, the methylaspartase system has been regarded as the archetypal example of an enzyme which operates via a carbanion elimination mechanism, and indeed, recent studies of the related systems L-aspartase (Nuiry et al., 1984), phenylalanine ammonia-lyase (Hermes et al., 1985), and argininosuccinate lyase (Kim & Raushel, 1986) have revealed the operation of similar elimination mechanisms.

Scheme I

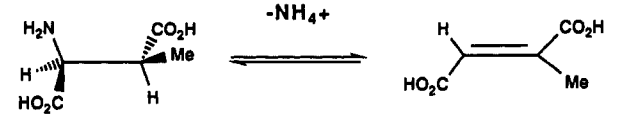

Research in our own laboratories led us to investigate the kinetics of the methylaspartase system using a range of substrate analogues (Akhtar et al., 1987; Botting et al., 1988a) and, furthermore, prompted an examination of the primary

† This work was supported by Science and Engineering Research Council Grants GR/D-63400 and GR/E-44673 to D.G. Some of the work described here was carried out at the Department of Chemistry, The University, Southampton SO9 5NH, U.K., and is a contribution from the Institute of Biomolecular Science at the University of Southampton, a Molecular Recognition Research Centre.

* To whom correspondence should be addressed.

0006-2960/92/0431-1509$03.00/0

deuterium isotope effects for the deamination of these substrate analogues (Botting et al., 1988b). To our surprise, (2*S*,3*S*)-3-methylaspartic acid, the physiological substrate, showed a significant isotope effect of ~1.7 on V and V/K over a wide pH range, in complete contrast to the reported findings (Bright, 1964). While the deuteriated substrate in Bright's experiments (conditions not specified) contained up to 13% unlabeled material, we were reluctant to believe that this level of contamination was sufficient to cause the complete masking of the isotope effect. In view of our own findings, we were also reluctant to leave the carbanion mechanism unchallenged.

In this paper we describe the results of experiments to define the kinetic mechanism of the enzyme, probe the binding order and the roles of the monovalent and divalent cations, and also present evidence to show that C-3 hydrogen exchange does not occur at the level of the putative carbanion intermediate.

Materials and Methods

Materials. Tris(hydroxymethyl)aminomethane (Tris),[1] magnesium chloride hexahydrate, and deuterium oxide (99.8 atom %) were obtained from Sigma Chemical Co. (St. Louis, MO). Potassium chloride was obtained from British Drug Houses (Poole, Dorset, U.K.). Tritiated water was combined from Amersham International (Amersham, Bucks, U.K.). [^{15}N]Ammonium chloride (99 atom % ^{15}N) was obtained from MSD Isotopes (Montreal, Canada). Water-miscible scintillant (ES-199) was obtained from Canberra Packard (Pangbourne, Berks, U.K.). (2*S*,3*S*)-3-Methylaspartic acid and (2*S*,3*S*)-[3-^{2}H]-3-methylaspartic acid were prepared as previously reported (Botting et al., 1987; Akhtar et al., 1987). All batches of the deuteriated substrate contained >95 atom % deuterium at the 3-position. All other chemicals were of analytical grade or were purified before use.

Enzyme. 3-Methylaspartate ammonia-lyase was purified from *Clostridium tetanomorphum* strain H1 (ATCC 15920), obtained from the American Type Culture Collection, grown according to the method of Barker et al. (1959) with a modification of literature procedures (Barker et al., 1959; Hsiang & Bright, 1969) as previously described (Botting et al., 1988). The specific activity of the enzyme used in these studies was 25–40 units (mg of protein)$^{-1}$.

Enzyme Assay. Enzyme was assayed according to the method of Barker, where 1 unit of enzyme catalyzes the formation of 1 μmol of mesaconic acid min^{-1} at pH 9.0 at 30 °C as determined by the increase in OD_{240} under the assay conditions (Barker et al., 1959).

Determination of Kinetic Parameters for Deamination. Experiments were performed where pH, [Mg^{2+}], [K^+], and [substrate] were each varied. Some of these experiments were repeated with (2*S*,3*S*)-[3-^{2}H]-3-methylaspartic acid. The results of these were used to analyze the kinetic properties of the species and their binding order in the formation of the quaternary complex, E·S·Mg·K. Other experiments were performed in order to determine the debinding order of the products and the effects of inhibitors and activators. Essentially initial rate assays were conducted as described previously (Botting et al., 1988a). Each rate measurement was carried out in triplicate. All incubations were performed at 30 ± 0.1 °C and reactions were followed directly spectrophotometrically at 240 nm, on a Pye-Unicam SP8-500 instrument, under the stated conditions. Reactions were linear over the time course measured (up to 5% of total conversion). The initial rate data obtained were analyzed by nonlinear regression analyses using the commercially available computer program Enzfitter (Leatherbarrow, 1987).

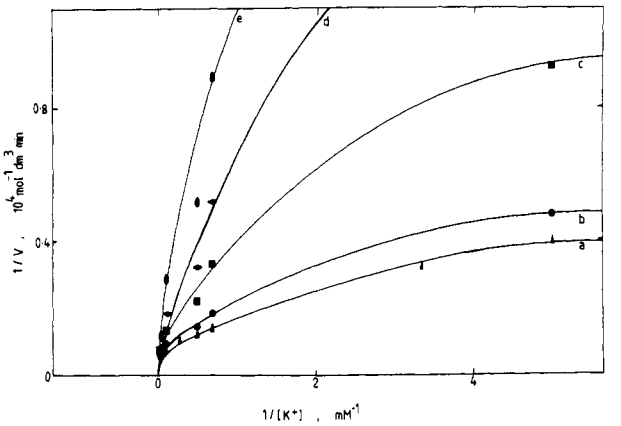

FIGURE 1: Variation of rate with potassium ion concentration. Incubations contained 0.5 M Tris (pH 9.0), 20 mM $MgCl_2$, 3-methylaspartic acid, and KCl in a total volume of 3 mL. Reactions were carried out at 30 ± 0.1 °C and corrected for 1 unit of enzyme. Traces are hand-drawn. (a) Infinite (see Discussion section); (b) 10 mM, (c) 2.0 mM, (d) 1.0 mM, and (e) 0.5 mM 3-methylaspartic acid.

Interpretation and Fitting of Initial Rate Data. A full analysis of the binding modes for the formation of the quaternary complex E·Mg·S·K was performed for each set of conditions using the method of Viola and Cleland (1982). The method uses the most general form of the rate equation for a terreactant system with species A, B, and C, assuming linear reciprocal plots:

$$v = VABC/(\text{constant} + aA + bB + cC + K_aBC + K_bAC + KcAB + ABC) \quad (1)$$

where a, b, and c are coefficients for A, B, and C, respectively, A, B, and C are reactant concentrations, K_a, K_b, and K_c are the corresponding Michaelis constants, BC, AC, and AB are the binary complex concentrations, and ABC is the concentration of the ternary complex.

Methylaspartase under some conditions does not show linear reciprocal plots for all species (Figure 1), for example, for K^+ at pH 9.0 (vide supra), so that the quantitative determination of all of the binding constants and terms is precluded. However, the linear asymptotes of the reciprocal plots for K^+ at high and low [K^+] can be used to determine which species are present under the two extreme conditions (Figure 1).

The method requires plotting the slopes and intercepts of reciprocal plots of initial rate versus C against $1/A$ and then plotting the slopes and intercepts of these plots against $1/B$ and determining the slopes and intercepts. The equations and methods are fully described in the original paper (Viola & Cleland, 1982). A table of replots for the values of the three slopes and intercepts is provided in a form associated with single terms in the denominator of eq 1 so that each term can be checked for its presence or absence.

To implement the method of analysis, K^+ was designated species C [because K^+ appeared to reduce observable isotope effects by increasing forward commitments (see discussion below)] and methylaspartic acid and Mg^{2+} were designated species A and B. The incorrect designation of species A and B does cause complications, but the identification of K^+ as species C simplifies the analyses because the $1/v$ versus $1/C$ plots are curved. Using the high and low [K^+] asymptotes to

[1] Abbreviations: NMR, nuclear magnetic resonance; UV, ultraviolet; TLC, thin-layer chromatography; Tris, tris(hydroxymethyl)aminomethane; Bis-tris propane, 1,3-bis[tris(hydroxymethyl)methylamino]-propane; ppm, parts per million (δ); GCMS, gas chromatography mass spectrometry; SIR-GCMS, single ion recording gas chromatography mass spectrometry.

produce two sets of slopes and intercepts for each K^+ concentration extreme, where each set is independently further processed, removed the problem of nonlinearity at the earliest stage. Graphs are presented in double-reciprocal form.

Cooperative Effect of Potassium Ion. Initial rate versus potassium ion concentration data gave sigmoidal plots. The reciprocal form gave curved, concave-down plots. The data were fitted to a negative cooperativity model. This was constructed on the basis of the results of the binding order studies and the isotope effect determinations described in this paper. The schemes and rate equations for fitting the data are described in the Discussion section.

Tritium Exchange. The rate of exchange was measured as the rate of tritium incorporation into the substrate. Thus (2*S*,3*S*)-3-methylaspartic acid (100 mM) was incubated at 30 ± 0.1 °C in tritiated water (activity ca. 2×10^8 dpm mL^{-1}) containing 500 mM Tris (pH 9.0), 20 mM $MgCl_2$, and 1 mM KCl in a total volume of 5 mL. Reaction was initiated by addition of preassayed enzyme solution (~0.3 unit). Aliquots (200 μL) were removed at timed intervals and quenched in acid (HCl, 0.1 M, 1 mL). The reactions were followed up to 5–10% of complete deamination, as judged by measurement of the optical density at 240 nm. Each aliquot was then diluted with water (20 mL) and was lyophilized. The residue was redissolved in water (20 mL) and was again lyophilized. The process was repeated to constant radioactivity, due only to tritium incorporated into the nonvolatile 3-methylaspartic acid. The final residue was dissolved in water (2 mL), scintillant was added, and the amount of tritium incorporated into the sample was determined by scintillation counting. Similar incubations using (2*S*,3*S*)-[3-^{2}H]-3-methylaspartic acid were performed.

Ammonia and Fumarate Trapping Experiments. [3-$^2H_3$]Mesaconic acid was prepared by literature methods (Thomas, 1990); mp 200–202 °C; δ_H (270 MHz, ^2H_2O) 6.61 (1 H, s, 2-H); δ_C (67.9 MHz, ^2H_2O) 125.41 (3-C), 141.31 (2-C), 167.89, 168.98 (1-C, 4-C). Anal. Calcd for $C_5H_6O_4$: C, 45.06; H, 4.54. Found: C, 45.06; H, 4.51.

(2*S*,3*S*)-3-Methylaspartic acid (2.85 mM) was deaminated in the presence of [3-$^2H_3$]mesaconic acid (7 mM), [^{15}N]ammonium chloride (7.7 mM), $MgCl_2$ (20 mM), KCl (1.0 mM), and Tris (500 mM, pH 9.0), in a total volume of 5 mL, at 30 ± 0.1 °C. Reaction was initiated by the addition of enzyme solution (~0.3 unit). Aliquots (200 μL) were removed at various time intervals and were quenched with concentrated hydrochloric acid (200 μL). A solution of glutamic acid (20 μL, 5 mg mL^{-1}) was added as an internal standard, and the solution was evaporated to dryness. The residue was dissolved in water (0.5 mL) and chromatographed on preparative cellulose TLC plates using isopropyl alcohol–aqueous ammonia (sp gr 0.88)–water (26:6:5) as eluant. The ninhydrin-positive bands were removed as one fraction and were extracted from the cellulose using methanol–water (1:1, 25 mL).

The cellulose was removed by filtration, the solvent was removed in vacuo, and the residue was dissolved in ethanol–water–triethylamine (5:2:3, 10 mL). Phenyl isothiocyanate (200 μL) was added to the stirred solution at 50 °C, and reaction was allowed to proceed for 30 min, after which time the solvent was removed in vacuo. The residue was redissolved in aqueous hydrochloric acid (1.0 M, 10 mL) and was stirred for a further hour at 50 °C. The aqueous reaction mixture was extracted with dichloromethane (3 × 30 mL), the pooled organic extracts were dried ($MgSO_4$), and the solvent was removed in vacuo. [A sample of the 3-methylaspartic acid phenylthiohydantoin derivative purified at this stage from a larger scale preparation gave the following spectral data: IR (Nujol) ν_{max} 3280 (N–H), 1770, 1740 cm^{-1} (C=O); δ_H (90 MHz, C^2HCl_3) 7.3 (5 H, m, ArH), 4.6 (1 H, d, J = 3.5 Hz, 2-H), 3.05 (1 H, m, 3-H), 1.34 (3 H, d, J = 7.6 Hz, 3-Me); EI-MS m/z (rel intensity, assignment) 264 (100, M^+), 135 (60, $PhNCS^+$), 77 (55, $C_5H_5^+$).]

The residue was dissolved in methanol–chloroform (2:23, 1 mL) and was treated with ethereal diazomethane (200 μL). The mixture was then analyzed by SIR-GCMS to determine the ratios of the isotopomers. The analyses were performed on a VG Analytical 70-250-SE mass spectrometer interfaced to a Hewlett-Packard 5790A gas chromatograph fitted with a 12M BP1-025 fused silica capillary column. The mass spectrometer was operated in EI mode (70 eV; 8 kV; R = 1000), with the interface and ion source at 280 and 200 °C, respectively. Splitless injections (2 μL) were employed using an injector temperature of 220 °C and an initial column temperature of 35 °C. The column was held at this temperature for 2 min, increased to 200 °C at 25 °C min^{-1}, then to 230 °C at 4 °C min^{-1}, and finally to 300 °C at 25 °C min^{-1}. Nominal masses 291–298, M − H to M + H for the unlabeled and doubly labeled species, respectively, were monitored. Thus, any contribution from the loss of a hydrogen atom from the labeled moieties could be taken into account. Peak areas for the different labeled species were recorded, normalized with respect to the internal standard, and corrected for the M − H contribution and natural isotopic abundances. This was achieved by repeatedly obtaining spectra of the authentic purified phenylthiohydantoin derivatives to determine accurate values for the contribution from the $(M - H)^+$, $(M + 1)^+$ and $(M + 2)^+$ ions. These values were used to correct the intensities of the ions obtained in spectra of the mixtures of derivatives (see Figure 1 in supplementary material).

Note that GCMS analysis of the purified 3-methylaspartic acid phenylthiohydantoin derivative, treated as above, indicated that the thiohydantoin ring and the carboxylic acid had been methylated: EI-MS m/z (rel intensity, assignment) 292 (20, M^+), 233 (100, $[M - CO_2Me]^+$), 205 (38, $[M - CH(Me)CO_2Me]^+$), 150 (75, $PhN(Me)CS^+$), 135 (35, $PhNCS^+$), 77 (45, $C_5H_5^+$). [^{1}H-NMR spectroscopic analysis ($CDCl_3$, 360 MHz) indicated that *S*- and *N*-thiohydantoin ring methylation had occurred to approximately equal extents. Since the isomers did not separate under the GC conditions employed and since only the parent ions were to be monitored, see below, the presence of isomers does not complicate the analysis.] The corresponding authentic trideuteriomethylaspartic derivative showed EI-MS m/z (rel intensity, assignment) 295 (65, M^+), 236 (100, $[M - CO_2Me]^+$), 205 (35, $[M - CH(CD_3)CO_2Me]^+$), 150 (40, $PhN(Me)CS^+$), 135 (15, $PhNCS^+$), and 77 (22, $C_5H_5^+$) (Figure 1 in supplementary material). The methylated phenylthiohydantoin derivative of glutamic acid was used as a calibration standard and showed EI-MS m/z (rel intensity, assignment) 292 (90, M^+), 260 (35, M^+ − MeOH), 218 (100, $M^+ - CH_3CO_2Me$), 135 (35, $PhNCS^+$), and 77 (38, C_5H_5). The compound was well separated on GC from the methylaspartic acid derivatives.

Results

Substrate, Potassium Cation, and Magnesium Cation. The potassium ion concentration dependencies of the kinetic parameters K_m (K_{MeAsp}) and V_{max} for unlabeled and 3-deuteriated (2*S*,3*S*)-3-methylaspartic acid at pH 9.0 and at 20 mM Mg^{2+} are shown in Table I. $^DV_{MeAsp}$ and $^D(V/K)_{MeAsp}$ vary synchronously over the studied conditions and there is no isotope effect on K_m, the value of which decreases with increasing $[K^+]$. The values of $^DV_{MeAsp}$ and $^D(V/K)_{MeAsp}$ of 1.7 are

Table I: Variation of Kinetic Parameters for (2*S*,3*S*)-3-Methylaspartic acid with Potassium Concentration[a]

	(2*S*,3*S*)-3-methylaspartic acid		(2*S*,3*S*)-[3-^{2}H]-3-methylaspartic acid			
[KCl] (mM)	K_M (mM)	V_{max}[b] (10^{-6} mol dm^{-3} min^{-1})	K_M (mM)	V_{max}[b] (10^{-6} mol dm^{-3} min^{-1})	^DV	$^D(V/K)$
0.2	2.42 ± 0.9	249	2.59 ± 0.5	209	1.19	1.27
0.3	2.80 ± 0.8	309	2.63 ± 0.5	274	1.13	1.06
1.6	2.37 ± 0.2	654	2.35 ± 0.25	385.2	1.70	1.68
3.0	1.78 ± 0.05	708	1.79 ± 0.09	533	1.33	1.34
4.0	1.50 ± 0.1	764	1.51 ± 0.26	633	1.21	1.21
10.0	1.26 ± 0.2	1191				
50.0[c]	0.67 ± 0.07	2089	0.67 ± 0.07	2089	1.00	1.00

[a] Incubations contained 0.5 M Tris (pH 9.0), 0.02 M $MgCl_2$, and substrate and KCl, in a total volume of 3 mL. Reactions were run at 30 ± 0.1 °C. [b] Corrected for 1 unit of enzyme assayed at pH 9.0. Error on V_{max} values is ±10%. [c] Both isotopomers lie on the same on plot.

Table II: Variation of Kinetic Parameters for (2*S*,3*S*)-3-Methylaspartic Acid with Magnesium Concentration[a]

	(2*S*,3*S*)-3-methylaspartic acid			(2*S*,3*S*)-[3-^{2}H]-3-methylaspartic acid				
[$MgCl_2$] (mM)	K_M (mM)	V_{max}[b]	V/K	K_M (mM)	V_{max}[b]	V/K	^DV	$^D(V/K)$
0.2	0.60 ± 0.10	175	292					
0.4	0.96 ± 0.05	301	314	0.93 ± 0.08	262	282	1.15	1.11
1.0	1.09 ± 0.09	350	321	1.12 ± 0.05	235	210	1.49	1.53
20.0	2.37 ± 0.2	654	276	2.35 ± 0.25	385.2	164	1.70	1.68
100.0	7.98 ± 0.9	341	43	8.32 ± 0.6	326	39	1.05	1.10
0.4[c]	0.40 ± 0.04	1227	3068					
1.0[c]	0.42 ± 0.03	1392	3164					
20.0[c]	0.67 ± 0.07	2089	3118					

[a] Incubations contained 0.5 M Tris (pH 9.0), 1.6 mM KCl, substrate, and magnesium chloride in a total volume of 3 mL. Reactions were run at 30 ± 0.1 °C. [b] 10^{-6} mol dm^{-3} min^{-1}; corrected for 1 unit of enzyme assayed at pH 9.0. Error ± 10%. [c] Incubations as above but containing 50 mM KCl.

maximal at ~1 mM K^+. At both higher and lower [K^+] the magnitudes of the apparent isotope effects decrease (Figure 2 in supplementary material). In a similar manner, at pH 6.5, the values of $^DV_{MeAsp}$ and $^D(V/K)_{MeAsp}$ decreased from 1.7 at 1.2 mM K^+ to 1.0 at 50 mM K^+.

At pH 9.0, in the presence of 4 mM substrate, the double-reciprocal plot for initial rate versus [K^+] is curved, concave down. The corresponding plots at pH 7.6 and 6.5 are linear. The high [K^+] asymptote of the pH 9.0 plot is linear and intersects with the pH 7.6 and pH 6.5 lines at infinite [K^+]. The values of the apparent dissociation constant for potassium ion, K_K, decrease markedly with increasing pH (Figure 3 in supplementary material) and H^+ acts as an apparent competitive inhibitor.

At pH 9.0, plots for experiments conducted over a range of substrate concentrations intersected at $1/V_{max}$, indicating rapid equilibrium substrate binding. Again using the linear high [K^+] asymptote of the pH 9.0 plots, the values of ^DV_K and $^D(V/K)_K$ were determined to be 1.0 and >1.25, respectively, and to be independent of substrate concentration. The curvature of the plot at lower [K^+] precluded further simple interpretation; see Discussion section.

At pH 9.0, in the presence of 1 mM substrate, the apparent values for the dissociation constant for Mg^{2+}, K_{Mg}, were similar at 1.6 and 50 mM K^+ (Figure 4 in supplementary material). The Mg^{2+} concentration, likewise, did not affect the value of K_K at any given substrate concentration.

The magnesium ion concentration dependencies of the kinetic parameters K_m and V_{max} for unlabeled and 3-deuteriated (2*S*,3*S*)-3-methylaspartic acid at pH 9.0 and at 1.2 mM K^+ are shown in Table II. $^DV_{MeAsp}$ and $^D(V/K)_{MeAsp}$ increase synchronously with increasing Mg^{2+} to a maximum value of 1.7 and there is no isotope effect on K_{MeAsp}, which increases with increasing Mg^{2+}. The data obtained at 100 mM Mg^{2+} show the occurrence of substrate inhibition. The double-reciprocal plots of initial rate versus [MeAsp] at different divalent metal ion concentrations are parallel (Figure 5 in supplementary material) (indicating the absence of the [K^+] term in the denominator of the rate equation; see Discussion section) both at 1.6 and at 50 mM K^+. However, V/K for the experiments conducted at 1.6 mM K^+ is ~10-fold lower than for those conducted at 50 mM K^+. In contrast to the situation at pH 9.0, at pH 7.6 and at 1.6 mM K^+, double-reciprocal plots of initial rate versus [S] at different divalent metal ion concentrations ([Mg^{2+}] = 20, 5, and 0.4 mM) intersect on the vertical axis (at infinite [S]) (see supplementary material Figure 6A). Thus, the [K^+] term is present in the denominator of eq 1, Mg^{2+} adds in rapid equilibrium and K_{iMg} = 0.75 mM. At pH 6.5 in the presence of 50 mM K^+, double-reciprocal plots of initial rate versus [S] at different divalent metal ion concentrations also intersect ([K^+] term present) but at finite substrate levels (Figure 6B in supplementary material). Note that the 0.2 mM line is parallel to the 0.4 mM Mg^{2+} line, so that at lower [Mg^{2+}] the [K^+] term in eq 1 vanishes.

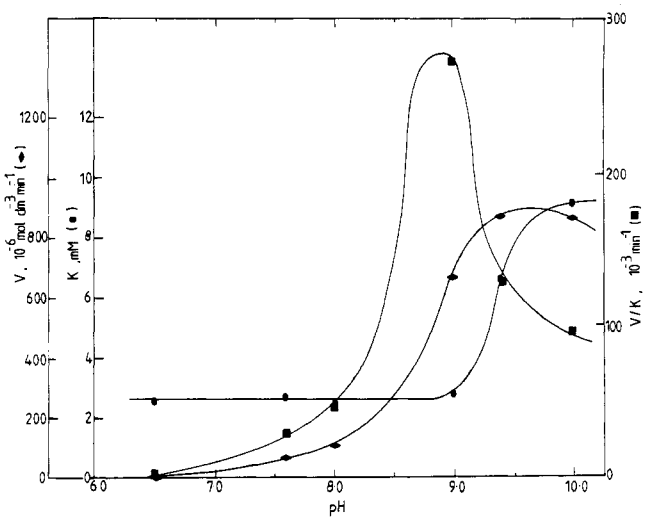

FIGURE 2: pH profile for the deamination of 3-methylaspartic acid. Incubations contained 20 mM $MgCl_2$, 1 mM KCl, substrate, and buffer (0.5 M Tris for pH 7.6–10, 0.1 M Bis-tris propane for pH 6.5–7.6). Reactions were run at 30 ± 0.1 °C and corrected for 1 unit of enzyme.

Table III: Rates of Deamination and Tritium Exchange[a]

substrate	initial rates[b] (10^{-4} mol dm^{-3} min^{-1}) deamination[c]	exchange[d]	v_{ex}/v_{deam}	$^{D}(V/K)_{deam}$	$^{D}(V/K)_{ex}$
(i) pH 9.0					
(2*S*,3*S*)-3-methylaspartic acid	1.70	1.60	0.94		
(2*S*,3*S*)-[3-^{2}H]-3-methylaspartic acid	0.99	1.02	1.03	1.7	1.6
(ii) pH 7.6					
(2*S*,3*S*)-3-methylaspartic acid	1.44	7.35	5.10		
(2*S*,3*S*)-[3-^{2}H]-3-methylaspartic acid	0.895	4.97	5.55	1.6	1.5
(iii) pH 6.5					
(2*S*,3*S*)-3-methylaspartic acid	0.735	1.35	1.83		
(2*S*,3*S*)-[3-^{2}H]-3-methylaspartic acid	0.54	0.894	1.66	1.4	1.5

[a] Incubation mixtures contained 0.5 M Tris (pH 9.0), 0.02 M $MgCl_2$, 0.001 M KCl, and substrate in a total volume of 5 mL of tritiated water (ca. 2×10^8 dpm mL^{-1}). [b] Corrected for 0.25 unit of enzyme in 5 mL. [c] Measured by UV spectroscopy. [d] Measured by tritium "wash-in".

The pH dependencies of V_{max}, V/K, and K_m for substrate deamination at 1.6 mM K^+ and 20 mM Mg^{2+} are shown in Figure 2. The curve for V_{max} is bell shaped and is maximal at pH 9.7. K_m is pH independent below pH 9.0 but increases markedly above pH 9.0; consequently, the V/K profile is maximal at pH ~9.0.

Ammonium Ion and Mesaconate. The effects of ammonium ion on the kinetic parameters for substrate deamination at pH 9.0 in the presence of 20 mM Mg^{2+} are shown in Figure 7, panels A and B, supplementary material. In the presence of 1.6 mM K^+, ammonium ion acts as an activator and increases V/K. V_{max} is increased and K_m is decreased so that the effect of ammonium ion is very similar to that of K^+. At higher concentrations, increasing NH_4^+ gives rise to product inhibition and the analysis of the effects is complicated. However, at high [K^+] the activating effect of NH_4^+ is almost saturated, and double-reciprocal plots of initial rate versus [S] at different ammonium ion concentrations are almost parallel at low [NH_4^+] (0–100 mM) and convergent at high [NH_4^+], indicating that ammonium ion is probably a noncompetitive product inhibitor. Parallel patterns are not expected for product inhibitors, and an additional binding mode for NH_4^+ appears to be available; see Discussion section.

Methylamine is a weak linear competitive inhibitor for methylaspartic acid (K_i = 150 mM) in the deamination reaction (Figure 8 in supplementary material). Methylamine is also a weak linear competitive inhibitor for ammonia (K_i = 350 mM at 0.3 mM mesaconic acid) in the amination reaction direction (Figure 9 in supplementary material) and a linear competitive inhibitor for mesaconic acid (K_i = 90 mM at 50 mM NH_4^+). Methylamine does not act as an activator.

Ammonium ion acts as a substrate and as an activator in the amination reaction direction. The double-reciprocal plot for initial rate versus [NH_4^+] at pH 9.0 in the presence of 20 mM Mg^{2+} and 0.3 mM mesaconic acid is curved concave up (Figure 10A in supplementary material). Potassium ion acts as an activator in the amination reaction direction and increases V/K_{NH_4} but not V_{max}. The results are presented more clearly in double-reciprocal plots of the type initial rate versus [NH_4^+]^2 in Figure 10B in the supplementary material.

Double-reciprocal plots of initial rate versus [mesaconic acid] at different [NH_4^+] at pH 9.0 intersect at $-1/K_{Mes}$ on the horizontal; K_{Mes} = 1.24 mM (Figure 11 in supplementary material). The reverse replot, $1/v$ versus [NH_4^+]^2, also intersects on the horizontal; K_{NH_4} is 60 mM, and thus, the dissociation constant for each substrate is independent of the concentration of the other species.

(2*S*,3*S*)-3-Methylaspartic acid is a competitive inhibitor for mesaconic acid at pH 9.0; K_i = 3 mM.

C-3 Tritium Exchange. The C-3 hydrogen exchange reaction was investigated by measuring the rate of tritium wash-in into the substrate pool at high substrate concentration. Simultaneously, the rate of deamination was measured as an increase in optical density at 240 nm. The rates of hydrogen exchange (v_{ex}) and deamination (v_{deam}) and their ratios varied widely with pH; Table III. At high pH, v_{ex}/v_{deam} was small (~1.0) but it increased below pH 9.0 to a maximum of 5 at pH 7.6, below which the ratio became smaller.

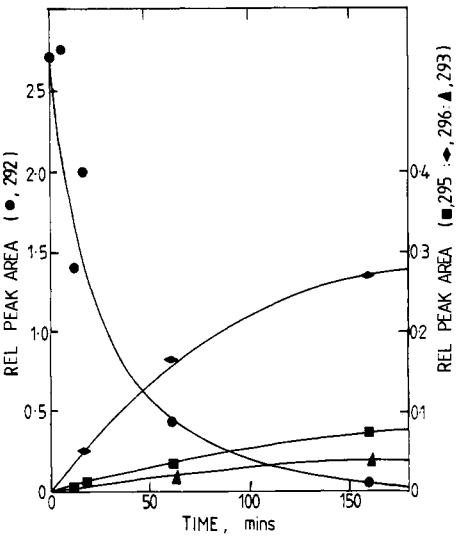

FIGURE 3: Data from ammonia trapping experiments. Incubations contained 2.85 mM 3-methylaspartic acid, 7 mM [*methyl*-$^2H_3$]mesaconic acid, [^{15}N]ammonium chloride, 20 mM $MgCl_2$, 1 mM KCl, 500 mM Tris (pH 9.0), and 0.3 unit of enzyme, at 30 ± 0.1 °C. For isolation, derivatization, and analysis procedures, see text. Traces are hand-drawn.

The primary isotope effects for the exchange and deamination reaction (effectively V_{max} ones) were determined by repeating the experiments with (2*S*,3*S*)-[3-^{2}H]-3-methylaspartic acid (Table III). The exchange reaction showed isotope effects of ~1.5 over the pH range studied and the values were similar to those for deamination. The magnitude of the isotope effect for the exchange reaction was, therefore, not dependent upon the ratio v_{ex}/v_{deam}, and $^{D}(v_{ex}/v_{deam})$ was close to unity over the entire pH range.

Product Trapping Experiments. The time course for the incorporation of ^{15}N-labeled ammonia and trideuteriomethylfumaric acid into a pool of unlabeled substrate, (2*S*,3*S*)-3-methylaspartic acid, under conditions where deamination is favored, is shown in Figure 3. The conversion of the unlabeled substrate to products proceeds most rapidly. In the amination direction the trace due to the formation of [^{15}N, *methyl*-$^2H_3$]methylaspartic acid (M_r of derivative = 296) increases most rapidly and is due, at least initially, to the direct addition of free labeled ammonia to free labeled mesaconic acid. The trace due to [*methyl*-$^2H_3$]methylaspartic acid (M_r

of derivative = 295) initially increases at about one-third of the rate for the doubly labeled species and at nearly twice the rate for [^{15}N]methylaspartic acid (M_r of derivative = 293). The rate of the formation of [^{15}N]methylaspartic acid is completely accounted for by the reaction of free labeled ammonium ion with free unlabeled mesaconic acid that has been formed through the deamination of unlabeled methylaspartic acid. The almost 2-fold faster rate of formation of [*methyl*-$^2H_3$]methylaspartic acid could indicate that unlabeled ^{14}N ammonium ion bound to the enzyme is, to some extent, trapped by free labeled mesaconic acid. However, under similar conditions the rate of C-3 hydrogen exchange with the solvent is faster than the deamination reaction and, thus, much faster than the rate of formation of either of the two singly labeled species. Therefore, neither unlabeled ammonia or unlabeled mesaconic acid is trapped on the enzyme.

Discussion

Early investigations of the kinetic mechanism of the L-*threo*-methylaspartase reaction by Bright and co-workers indicated that the enzyme operated via a carbanionic elimination mechanism. Their results were derived from the joint observations that the enzyme showed no primary deuterium isotope effect over a wide pH range (Bright, 1964), that C-3 hydrogen exchange with the solvent was as rapid or more rapid than the overall deamination reaction (Bright, 1964), and that the enzyme was capable of catalyzing the deamination of the L-*erythro* diastereomer of 3-methylaspartic acid (Bright et al., 1964b; Barker et al., 1959).

Recent work in our own laboratory revealed that there is a primary deuterium isotope effect for the deamination reaction with (2*S*,3*S*)-3-methylaspartic acid as the substrate (Botting et al., 1988b) and, therefore, it was necessary to determine why the isotope effect had not been detected previously.

Although the precise conditions for the attempted determination of the isotope effects had not been reported by previous workers (Bright, 1964), it was likely that the experiments were performed at a potassium ion concentration of at least 50 mM. Our experiments were performed at a much lower potassium ion concentration (Botting et al., 1988b). Since potassium is an activator for the deamination reaction, it seemed reasonable that its binding could cause an increase in the reaction commitments to the isotopically sensitive step. The activator could achieve this either by merely increasing the rate of the isotopically sensitive step relative to the substrate and product dissociation rates, by binding to the enzyme complex after the substrate in an ordered mechanism (thus retarding substrate dissociation), or by debinding before product release (thus retarding the rate of free enzyme formation). The effect of increased forward and/or reverse reaction commitments might then decrease the observed isotope effect toward unity. [For a review of reaction commitments see Cleland (1987).]

To test these possibilities, a series of kinetic isotope effect determinations were performed over a range of potassium concentrations. From the results (Table I), it was evident that both ^DV and $^D(V/K_{MeAsp})$ decreased toward unity with increasing monovalent cation concentration. Interestingly, ^DV and $^D(V/K_{MeAsp})$ varied synchronously (there was no effect on $^DK_{MeAsp}$) at pH 9.0 and at 6.5, from values of ~1.7 at a concentration of 1.6 mM potassium ion to unity at 50 mM potassium ion. The results at 50 mM potassium ion concentration compared to those at 1.6 mM, therefore, support the notion that the reaction commitments are increased and account for the failure of previous studies (Bright, 1964) to detect isotope effects. Nevertheless, the results give no clue as to whether the increases in commitments are due to rate enhancement, ordered binding, or both.

In isolation, the lack of an observable isotope effect on K_{MeAsp} (i.e., $^DV/^D(V/K) = 1$) at any given potassium concentration in the range studied, where there is an isotope effect on V/K, might be interpreted to suggest that the chemical steps are slow compared to the dissociation rates of the substrate and both products. Identical values for ^DV and $^D(V/K_{MeAsp})$ could indicate that there are no reaction commitments. The observation of rapid equilibrium substrate binding in the high [K^+] regime (see Results section) might be used to support this idea, while the variance of the values of ^DV and $^D(V/K)$ with potassium ion concentration is consistent with an ordered binding mode where the forward commitments (c_f and c_{vf} for the isotope effects on V/K and V, respectively) and the reverse commitment (c_r) are increased approximately equally with increasing potassium ion concentration. Thus, the magnitude of the observed isotope effects might be controlled solely by external commitments due to ordered K^+ binding. [See Cleland (1987) for the definition of reaction commitments.] However, there were many inconsistencies in the analysis (for example, why do ^DV and $^D(V/K)$ decrease at very low [K^+] and why do ^DV and $^D(V/K)$ decrease at very high [K^+] if the substrate binds in rapid equilibrium?) and it was not possible to determine the values of the reaction commitments or their origin until the binding and debinding orders of the metal ions, substrate, and products were known.

Substrate and Metal Ion Binding Orders. Considerable support for the notion that the binding order is compulsory (enzyme binds K^+ after MeAsp) was provided by the fact that no isotope effect for V or for V/K_{MeAsp} was detected at pH 6.5 at 50 mM potassium ion. Under these conditions, the apparent value of V^{app} is very low, ~10 times lower than its value at pH 9.0 at 1.6 mM potassium, where $^DV = ^D(V/K) = 1.7$. Hence, for a nonordered mechanism one might expect to observe isotope effects of at least 1.7.

While the values of ^DK_m were not affected by the concentration of potassium ion in the work at pH 9.0 (Table I), the apparent values of the Michaelis constants for the protio and deuterio substrates decreased considerably with increasing [K^+] and the double-reciprocal initial rate versus [S] plots did not intersect at a common point over the entire [K^+] range (Figure 2 in supplementary material). From 4 to 50 mM K^+, the plots did intersect at a common point above the x-axis where K_{iMeAsp} = 2 mM. On the other hand, at 3 mM K^+ there was no common point of intersection. At lower [K^+], plots intersected on the x-axis at ~2.4 mM. The complexities of the multiple points of intersection in the substrate dimension were mirrored in plots of initial rate versus [K^+]. These plots were sigmoidal while the reciprocal ($1/v$ versus $1/[K^+]$) plots were curved, concave down. Analysis of the reciprocal plots revealed a rapid equilibrium binding pattern for the substrate and an intersecting binding pattern for Mg^{2+} in the high [K^+] regime. Intersecting binding patterns were obtained for both species by extrapolation of the low [K^+] regime asymptotes. At 20 mM Mg^{2+}, the value of K_K at infinite [MeAsp], as estimated from the high [K^+] asymptote, was ~20.0 mM (Figure 1), and as estimated from the low [K^+] asymptote, the value was <0.5 mM.

In contrast, Bright had shown that at pH 5.1 (Bright, 1967) and at pH 7.0 (Fields & Bright, 1970) the values for the dissociation constant for K^+ (K_K) were 100 mM and 20 mM, respectively, and that the initial rate versus [K^+] plots were accurately hyperbolic over the concentration range 1–200 mM

Scheme II

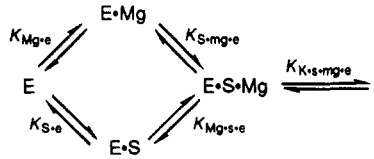

$$E•S•Mg•K \longrightarrow E + Mg + K + P + NH_4$$

potassium ion. Thus, the reciprocal plots were linear and obeyed the equation $v = V[K^+]/(K_K + [K^+])$. Under these conditions, at lower pH and at lower $[Mg^{2+}]$, only V^{app} and not V/K_{MeAsp} was affected by the potassium ion concentration, and therefore, the monovalent cation acted as a simple noncompetitive activator. [We obtained only slightly different results when Bright's experiments were repeated at pH 6.5 and 7.6 at 20 mM Mg^{2+}. The values of K_K were found to be 64 and 20 mM, respectively (Figure 6 in supplementary material), and K_{MeAsp} decreased slightly with increasing K^+ concentration.] Thus, the apparent mode of potassium ion activation was pH dependent.

Another puzzling feature of the effect of potassium concentration (at pH 9.0) was that the observed isotope effects for ^DV and $^D(V/K)$ were very small at low $[K^+]$, ~1.2 at 0.2 mM K^+ (Table I). The result is not easily accommodated in terms of K^+ binding to the enzyme after substrate in an ordered mechanism, as mentioned above, since reducing the forward commitment through decreasing $[K^+]$ should increase $^D(V/K)$ (Cleland, 1987). To explain the effect it was, therefore, necessary to examine the role of the other activator, Mg^{2+}.

The primary isotope effects for ^DV and $^D(V/K)$ were not affected by gross changes in the magnesium ion concentration (in the absence of substrate inhibition, at very high $[Mg^{2+}]$) except at very low $[Mg^{2+}]$ (Table II). Hence, it appeared that K^+, but not Mg^{2+}, was able to increase the reaction commitments at high concentration and that Mg^{2+} should be able to bind to the enzyme before the substrate.

Earlier workers had proposed that the enzyme should bind to the substrate and the divalent metal ion in a random fashion (Scheme II). However, the mode of K^+ binding had not been determined. In the light of the differences in the effects of the metal ion concentrations on the apparent primary isotope effect and the effect of pH on activation by K^+, it was necessary to determine the binding order leading to the active quaternary enzyme complex.

At 1.6 mM, and indeed also at 50 mM K^+, double-reciprocal plots of initial rate versus $[Mg^{2+}]$ gave a series of parallel lines when the substrate concentration was varied, corresponding to uncompetitive activation (Figure 5 in supplementary material). This result differed considerably from those obtained by Bright with Mg^{2+}, Co^{2+}, and Mn^{2+}, at saturating $[K^+]$ and at a lower pH (where K^+ acts as a simple noncompetitive activator), which showed intersecting substrate–M^{2+} patterns corresponding to mixed noncompetitive activation (Bright, 1965). These results were interpreted to indicate that the presence of substrate facilitated M^{2+} binding and that the divalent metal ion facilitated substrate binding. With Mg^{2+}, Co^{2+}, and Mn^{2+} as the divalent metal ion, each of the dissociation constants (K_m and K_i) was determined for each of the divalent metal ions and the substrate. Bright also demonstrated quite elegantly, through the use of kinetic and paramagnetic resonance relaxation techniques with the manganese enzyme at low pH, but in the absence of potassium ion, that the dissociation constants obtained from the kinetic work with Mg^{2+}, Co^{2+}, and Mn^{2+} were probably true dissociation constants (Bright, 1964, 1967; Bright & Silverman, 1964; Fields & Bright, 1967). On the basis of this work, the random order binding mechanism for substrate and magnesium was proposed (first part of Scheme II).

Scheme III

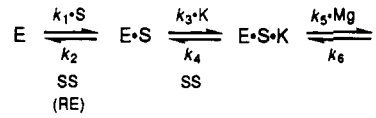

$$E•S•K•Mg \longrightarrow E + Mg + K + P + NH_4$$

Scheme IV

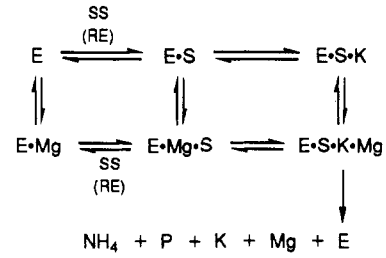

Scheme V

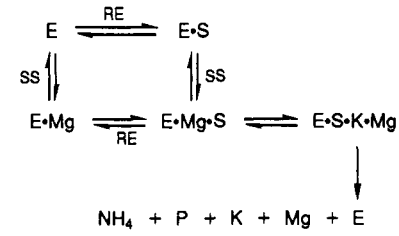

To rationalize the stark differences in the kinetic properties of methylaspartase under Bright's conditions and our own, a full analysis of the binding modes leading to the formation of the quaternary complex E•Mg•S•K was performed for each set of conditions using the method of Viola and Cleland (1982) and eq 2.

$$v = (V[MeAsp][Mg^{2+}][K^+])/(\text{constant} + a[MeAsp] + b[Mg^{2+}] + c[K^+] + K_{MeAsp}[Mg^{2+}][K^+] + K_{Mg}[MeAsp][K^+] + K_K[MeAsp][Mg^{2+}] + [MeAsp][Mg^{2+}][K^+]) \quad (2)$$

While simple analysis of the kinetic mechanism was precluded by the curved nature of the $1/v$ versus $1/[K^+]$ double-reciprocal plots, by using the high and low $[K^+]$ asymptotes for plots where the concentration of Mg^{2+} and substrate were varied, the two extreme conditions could be analyzed. Analysis of Bright's data, which were obtained at low pH (Bright, 1967; Fields & Bright, 1970), indicated that all of the terms should be present in rate equation 2. Since none of the species displayed rapid equilibrium binding patterns at low pH, the enzyme binds substrate and Mg^{2+} in a random steady-state (SS) fashion and then binds K^+ according to Scheme II (Viola & Cleland, 1982).

At pH 6.5, the decrease in the value of $^D(V/K)_{MeAsp}$ (see Results section) with increasing $[K^+]$ (caused by an increase in c_f) is consistent with this mechanism. If K^+ must be released before the first product, both c_r and c_{vf} would also increase with increasing $[K^+]$. Such a mechanism might account for the concomitant decrease in ^DV (see Results section).

At pH 9.0 the initial rate data indicate that at low $[K^+]$ the $c[K^+]$ term is missing in eq 2 and that at high $[K^+]$ the $c[K^+]$ and $K_{MeAsp}[Mg^{2+}][K^+]$ terms are missing. The results are

consistent with Schemes III and IV and Schemes III(RE), IV(RE), and V, respectively (SS = steady-state; RE = rapid equilibrium). In each of the schemes K^+ is unable to bind to the enzyme before the substrate. Thus, the size of c_f would be expected to increase, and therefore, the value of $^D(V/K)_{MeAsp}$ would be expected to decrease, with increasing $[K^+]$ regardless of the exact mechanism. This is observed (Table I).

Schemes in which Mg^{2+} can only bind after substrate [Schemes III and III(RE)] can be excluded as being the sole contributors given that the value of $^D(V/K)_{MeAsp}$ is not suppressed by increasing forward commitments with increasing $[Mg^{2+}]$. For a completely ordered mechanism, for example, for Scheme III, assuming only k_7 is affected by deuterium substitution in the substrate, the expected $[Mg^{2+}]$ and $[K^+]$ dependencies of $^D(V/K)$ are given by eq 3 and the external forward commitment ($c_{f\text{-}ex}$) is given by eq 4.

$$^D(V/K)_{MeAsp} = \{^Dk_7 + (k_7/k_6)[1 + (k_5[Mg^{2+}]/k_4) \times (1 + (k_3[K^+]/k_2))]\}/\{1 + (k_7/k_6)[1 + (k_5[Mg^{2+}]/k_4)(1 + (k_3[K^+]/k_2))]\} \quad (3)$$

$$c_{f\text{-}ex} = (k_2/k_6)\{1 + (k_5[Mg^{2+}]/k_4)(1 + (k_3[K^+]/k_2))\} \quad (4)$$

Indeed, the value of $^D(V/K)_{MeAsp}$ increases with increasing $[Mg^{2+}]$ (Table II), indicating that Mg^{2+} can bind before the substrate and, in so doing, rescues the substrate from following a high commitment pathway such as that embodied in eq 3. Hence, the existence of the species E·Mg^{2+} and E·Mg^{2+}·MeAsp in Schemes IV and IV(RE) provides a pathway in which the substrate can dissociate from the enzyme before Mg^{2+} does and in which only increasing $[K^+]$ can cause increasing commitments. The remainder of the scheme is identical to Scheme III and, as discussed above, predicts that increasing the concentration of either or both metal ions would increase c_f.

Since decreasing $[Mg^{2+}]$ causes the value of $^D(V/K)_{MeAsp}$ to decrease toward unity (Table II), it appears that the pathway depicted in Scheme III becomes more important at low $[Mg^{2+}]$ and K^+ binds second. Competition for E·MeAsp by K^+ with Mg^{2+} at increasing $[K^+]$, so that the MeAsp, then K^+, then Mg^{2+} binding pathway is favored [Scheme III(RE)] would account for the decrease in $^D(V/K)_{MeAsp}$ at high $[K^+]$. This is because only the completely ordered addition of at least two species to the binary enzyme complex of an equilibrium ordered substrate would be expected to increase the forward commitments to an extent sufficient to completely suppress an isotope effect on V/K. Note that MeAsp is only in rapid equilibrium at high $[K^+]$ (see Results section). At low $[K^+]$ the substrate adds in the steady state and could, potentially, dissociate slowly enough from its binary complex with the enzyme to preclude the observation of an isotope effect, regardless of the influence of the metal ions.

Given that when the substrate adds in rapid equilibrium it is K^+ which causes the forward commitments to increase and that at pH 9.0, as at lower pH, the metal ion always binds after the substrate, it is reasonable to ascribe the decreasing value of ^DV with either increasing $[K^+]$ or decreasing $[Mg^{2+}]$ (Tables I and II) to increased values of c_{vf} and c_r. For a symmetrical mechanism, the increases values of the commitments would be caused by the ordered release of K^+ from the enzyme–product complex prior to the release of other species.

Although our analysis rationalizes the kinetic behavior of the enzyme at low pH and at pH 9.0 in the high $[K^+]$ regime (where double-reciprocal plots of initial rate versus $[K^+]$ are linear from ~4 to 50 mM and where the substrate adds in rapid equilibrium), no explanation has emerged for the decreasing values of the substrate isotope effects or for the transition to steady-state substrate binding and the accompanying curvature in the reciprocal plots at low $[K^+]$. As alluded to above, when the substrate adds in the steady state and when the substrate is sticky, V/K isotope effects can be completely suppressed. However, the value of ^DV should not be affected since the value of V is much lower at low $[K^+]$ and, therefore, product release should not be rate limiting. Nevertheless, at low $[K^+]$ ^DV and $^D(V/K)_{MeAsp}$ decrease rapidly toward unity (Table I), and our explanation for the decreasing values of the isotope effects at high $[K^+]$ in terms of increased external commitments due to ordered K^+ binding, curiously, seems appropriate also to the decreasing values of the isotope effects at low $[K^+]$. Four results support this contention.

Scheme VI

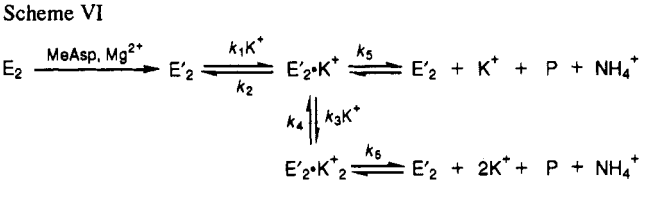

First, the allowed pathways leading to the formation of the quaternary complex at high $[K^+]$ [Schemes III(RE) and IV(RE)] and at low $[K^+]$ (Schemes III and IV) are similar. A transition to a high K^+ affinity form of the enzyme at low $[K^+]$, where K^+ dissociates very slowly, could, therefore, result in increased reaction commitments, as described above.

Second, the initial rate versus $[K^+]$ plots are sigmoidal and show two saturation curves which could indicate cooperativity effects. The $1/v$ versus $1/[K^+]$ plots are curved and the low $[K^+]$ linear asymptotes extrapolate to a very low value of K_K. Also, although V^{app} increases, $(V/K_K)^{app}$ decreases in progressing from low to high $[K^+]$. Reaction commitments and the "stickiness" of various species are known to increase as V/K is increased (Cleland, 1987), and for this reason isotope studies are often conducted with slow or loose substrate or at a pH away from the optimal.

Third, sequential termolecular enzyme mechanisms should not give parallel-line initial velocity patterns when the concentrations of two species are varied unless the other species is saturating. While parallel MeAsp–Mg^{2+} reciprocal plot patterns at pH 9.0 and at 50 mM K^+ (equivalent to ~3 times K_K) might be expected, the patterns at 1.6 mM K^+ should not be parallel unless, of course, a different form of the enzyme is responsible for catalysis and is saturated with K^+. This appears to be the case (Figure 5 in supplementary material).

Fourth, there is evidence to indicate that there are two active sites per A_2B_2 enzyme molecule (Wu & Williams, 1968; Hsiang & Bright, 1967, 1969), although there has been confusion regarding the exact subunit structure (Botting & Gani, 1989). Recent work in our laboratory has shown that the enzyme is an A_2 homodimer (S. Goda, N. Minton, N. P. Botting, and D. Gani, unpublished results). Thus, the enzyme could, potentially, display cooperativity effects.

To determine if cooperativity between the two active sites of methylaspartase could account for the curved initial rate versus $[K^+]$ plots, Scheme VI was devised. The scheme assumes that K^+ always binds after substrate and after Mg^{2+} and that both active sites are completely saturated with the first two species. This is a reasonable assumption at infinite substrate concentration and at 20 mM Mg^{2+} given the results of the binding order studies. Note that K_{MeAsp} is dependent on $[K^+]$ whereas K_{Mg} is not (Table I; Figure 4 in supplementary material).

The steady-state treatment of Scheme VI using the King–Altman method (King & Altman, 1956) gave eq 5, which

relates the initial rate, v, to $[K^+]$ in the absence of products:

$$v = \{e_0([k_5(k_4 + k_6)/k_3][K^+] + k_6[K^+]^2)\}/\{[(k_2 + k_5)/k_1][(k_4 + k_6)/k_3] + ([(k_4 + k_6)/k_3] + (k_6/k_1))[K^+] + [K^+]^2\} \quad (5)$$

In order to define the ratios of rate constants in terms of experimentally measurable parameters and set boundary conditions for the methylaspartase system, the apparently linear asymptotes of double-reciprocal plots at very low and very high $[K^+]$ were considered in terms of eq 5.

It was recalled that graphical analysis of the experimental data had indicated that K_K for the low $[K^+]$ regime (K_1) was at least 100-fold smaller than K_K for the high $[K^+]$ regime (K_2) and that V for the low $[K^+]$ regime (V_1) was $\sim^1/_6$ of V for the high $[K^+]$ regime (V_1) (i.e., $k_5/k_6 \sim 0.16$). From the kinetic model, the potassium ion k_{off} rate constants, k_2 and k_4, should be larger than k_5 and k_6, respectively, as defined in Scheme VI. This is because k_5 and k_6 are composite rate constants which contain catalytic as well as debinding steps for K^+ and the products. Within these boundaries and setting $K_1 = (k_2 + k_5)/k_1$, it is possible to show that k_6/k_1 is much smaller than $(k_4 + k_6)/k_3$ if the second-order rate constants k_1 and k_3 are similar in magnitude (or at least if k_3 is not much larger than k_1). This is true regardless of whether the terms $\{(k_4 + k_6)/k_3 + (k_6/k_1)\}$ or $(k_4 + k_6)/k_3$ are taken to represent K_2. Indeed, if $k_1 = k_3$ and k_5 is set to its maximum permissible value (equal to k_2), k_4 is at least 34 times larger than k_6 and the term k_6/k_1 in the denominator of eq 5 can be ignored without grossly affecting the model.

At very low $[K^+]$, all terms containing $[K^+]^2$ should be insignificant compared to the others. Thus, in the low $[K^+]$ regime, eq 5 would simplify to

$$v = \{e_0[k_5(k_4 + k_6)/k_3][K^+]\}/\{[(k_2 + k_5)/k_1] \times [(k_4 + k_6)/k_3] + ([(k_4 + k_6)/k_3] + (k_6/k_1))[K^+]\} \quad (6)$$

Where k_6/k_1 is much smaller than $(k_4 + k_6)/k_3$, eq 6 simplifies further to eq 7, which gives a linear reciprocal plot where $V_1 = e_0k_5$ and where the apparent dissociation constant for K^+ at low $[K^+]$, K_1, is equal to $(k_2 + k_5)/k_1$:

$$v = \frac{e_0k_5[K^+]}{\{(k_2 + k_5)/k_1\} + [K^+]} \quad (7)$$

At high $[K^+]$, terms that are not multiplied by $[K^+]$ become insignificant and eq 5 simplifies to

$$v = \frac{e_0\{[k_5(k_4 + k_6)/k_3][K^+] + k_6[K^+]^2\}}{\{[(k_4 + k_6)/k_3] + (k_6/k_1)\}[K^+] + [K^+]^2} \quad (8)$$

As argued above, k_6/k_1 should be much smaller than $(k_4 + k_6)/k_3$ and can therefore be discounted. Division of all terms of $[K^+]$ gives eq 9, which defines V_2, the rate at infinite $[K^+]$, as e_0k_6 and defines K_2, the first apparent dissociation constant for K^+ from $E'_2{\cdot}K^+_2$, as $(k_4 + k_6)/k_3$:

$$v = \frac{e_0\{[k_5(k_4 + k_6)/k_3] + k_6[K^+]\}}{[(k_4 + k_6)/k_3] + [K^+]} \quad (9)$$

Equation 9 does not have a linear reciprocal form unless k_5 is zero, which is not true here (see below). However, the reciprocal form approaches linearity at very high $[K^+]$ and allows the lower limit of K_2 to be estimated. The graphical analysis is greatly assisted because the value of V_2 does not need to be obtained from eq 9. The value of V_2 can be determined from the common crossover point of the linear reciprocal plots of initial rate versus [MeAsp] (that used to determine K_{iMeAsp}; see Figure 2 in supplementary material) at high but varied potassium ion concentrations. Therefore, its value can be entered on the x-axis of the v versus $[K^+]$ reciprocal plot at infinite $[K^+]$, and this practice reduces the length of the extrapolation required to estimate the upper limit of $-1/K_2$.

Table IV: Variance of Initial Rate with $[K^+]$ Fitted to Equation 10

variable	initial estimate[a]	fitted value
V_1	0.50[b]	0.59 ± 0.09
K_1	0.2 mM	0.28 ± 0.10
V_2	3.3[b]	3.40 ± 1.15
K_2	20 mM	33.40 ± 3.52
σ[c]	0.0036	

[a] Estimates from graphical analysis. [b] Units are mmol dm^{-3} min^{-1}. [c] $\sigma = [\sum(\text{experimental velocity} - \text{theoretical velocity})^2/\text{no. of data points} - n]^{1/2}$ where n equals the number of terms in the denominator. Other tested models did not converge; see Discussion section.

This estimate, together with those of V_1, V_2, and K_1, were then fitted to the experimentally derived maximum velocities at infinite [MeAsp] and at 20 mM Mg^{2+} using

$$v = \frac{V_1K_2[K^+] + V_2[K^+]^2}{K_1K_2 + K_2[K^+] + [K^+]^2} \quad (10)$$

A good fit was obtained (see Table IV). To verify that the presence of a catalytically active form of E'_2K^+ existed, the data were also fitted to eq 11, which corresponds to Scheme VI in which k_5 is set equal to zero:

$$v = \frac{V_2[K^+]^2}{K_{i1}K_2 + K_2[K^+] + [K^+]^2} \quad (11)$$

No convergence was obtained. A model in which V_1 was set equal to V_2 (i.e., $k_5 = k_6$ in Scheme VI) also failed to converge. Thus the enzyme appears to operate via two catalytically competent species, E'_2K^+ and $E'_2K^+_2$, which differ in their abilities to debind K^+ and to convert substrate to products. The joint findings that the affinity of the enzyme for the first potassium ion to bind is more than 100-fold greater than that for the second and that E'_2K^+ is catalytically active and must bind to the substrate before potassium ion are completely consistent with the variance of the observed isotope effects as discussed above.

Hence, as the $[K^+]$ is reduced from 50 mM toward 1 mM, the reaction commitments decrease [Scheme IV(RE)] and isotope effects are observed. Below 1 mM K^+, very little of the enzyme exists in the $E'_2K^+_2$ form and a new catalytic form (E'_2K^+) with different kinetic properties (high K^+ affinity, substrate binds in the steady state) dominates the mechanism (Schemes III and IV).

Given that the binding order for the substrate and metal ions had been determined as a function of pH, the rationalization of the complicated effects of ammonium ion on the system could commence. Three observations needed to be considered.

First, it had been shown that at very low $[K^+]$ the enzymic reaction behaved autocatalytically (Barker et al., 1959). In our work at 0.2 mM K^+, reciprocal initial rate versus [MeAsp] plots were not curved, indicating that autocatalysis does not complicate the analysis of the results described in this paper. However, we were able to show that the rate of conversion of substrates to products increased with respect to time if no K^+ was included in the incubation solution. While it was clear that the release of the product ammonium ion would allow the cation to act as an efficient surrogate for K^+ at the activator site, that presented by E·MeAsp or E·MeAsp·Mg^{2+} (Schemes

Scheme VII

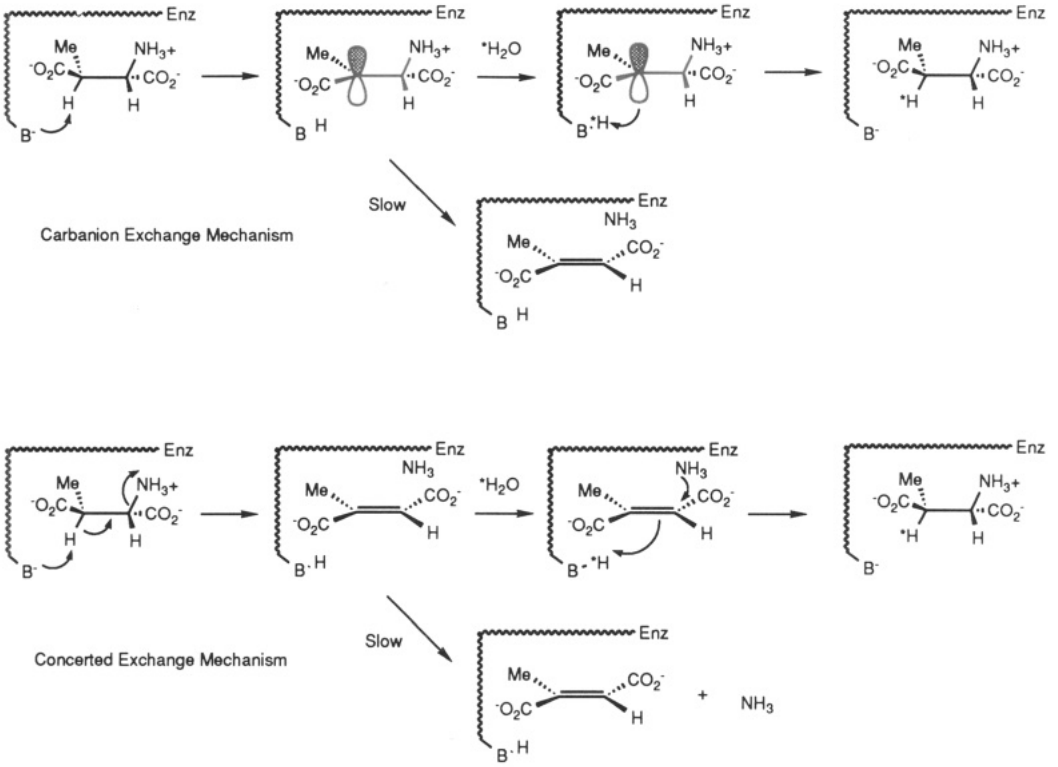

III and IV), it was not known how the free enzyme might interact with ammonium ion as a product.

Second, it was known that ammonium ion, but not K^+, could enhance the rate of a side reaction, substrate C-3 hydrogen exchange with the solvent, over that for normal deamination (Bright, 1964). The debinding order for the products, mesaconic acid and ammonium ion, was not known, but the third observation ruled out the simple back reaction as a cause of the increased exchange to deamination ratio, v_{ex}/v_{deam}.

In this experiment, Bright showed that when [^{15}N]ammonia was used to enhance the ratio v_{ex}/v_{deam}, ^{15}N label was not incorporated into the C-3 hydrogen-exchanged substrate pool (Bright, 1964). Thus, it appeared as though the increase in v_{ex}/v_{deam} was caused without breakage of the C–N bond. The result was used to argue in favor of a carbanionic elimination mechanism on the basis that the exchange of the proton from the substrate could then occur at the carbanion level before C–N bond cleavage, vide supra.

In view of the fact that no isotope effects had been observed for the forward reaction at that time and that it was reported that the enzyme could process the L-*erythro* diastereomer of the substrate to give mesaconic acid, the evidence in favor of a carbanion mechanism was compelling. Nevertheless, the recent observation of primary deuterium isotope effects for the deamination reaction (Botting et al., 1988b) called the existence of a long-lived solvent-accessible carbanion into question.

The exchange reaction was investigated by measuring tritium wash-in into the substrate pool at high substrate concentration. Simultaneously, the rate of deamination was measured as an increase in optical density at 240 nm (see Materials and Methods). The rates of exchange and deamination and the ratios of their rates varied widely with pH (Table III). At high pH, v_{ex}/v_{deam} was small, but it increased below pH 9.4 to a maximum of 5 at pH 7.6, below which the ratio became smaller.

The primary isotope effects for the exchange and deamination reaction (effectively effects on V_{max}) were determined by repeating the experiments with (2*S*,3*S*)-[3-^{2}H]-3-methylaspartic acid (Table III). It was immediately evident that the exchange reaction showed an isotope effect and that the magnitude of the effect was not dependent upon the ratio v_{ex}/v_{deam}, that is, $^D(v_{ex}/v_{deam})$ was close to unity over the entire pH range. These results strongly suggest that exchange occurs after a slow step which follows C–H bond cleavage. ^DV isotope effects are extremely sensitive to slow steps subsequent to the isotopically sensitive step. Evidently, in this case, where the ratio v_{ex}/v_{deam} changes so drastically, the observed isotope effect $^D(v_{ex})$ would also change, if exchange occurred freely at the carbanion level.

While these data tend to preclude free exchange of the substrate-derived hydrogen directly at the carbanion level, the results do not rule out a carbanionic mechanism. Scheme VII depicts possible exchange mechanisms for balanced stepwise carbanionic and concerted elimination processes.

Given that C-3 hydrogen exchange does not occur at the carbanion level and that increasing [NH_4^+] (but not [K^+]) increases the ratio v_{ex}/v_{deam} but does not lead to the incorporation of the added ammonium ion into the substrate pool, the added ammonium ion could not act by simple product inhibition. In order to delineate the exchange mechanism, the mode of product release for 3-methylaspartase was addressed.

Mesaconic acid acted as a competitive inhibitor for (2*S*,3*S*)-3-methylaspartic acid (K_i = 3 mM). For uni-bi mechanisms, this result indicates that the binding order for the substrates in the reverse reaction is random or that mesaconic acid adds first in a compulsory order scheme (Fromm, 1975).

The effects of adding ammonia as a product inhibitor were complex. At low [K^+], ammonium ion initially acted as an activator, increasing V^{app} and $(V/K)^{app}$ for the substrate (Figure 7A in supplementary material). The activator effect was very similar to that observed for increasing [K^+]. At higher ammonium ion concentration, the product began to inhibit in a noncompetitive manner. In order to suppress the effect due to activation by ammonium ion, a set of product

Scheme VIII

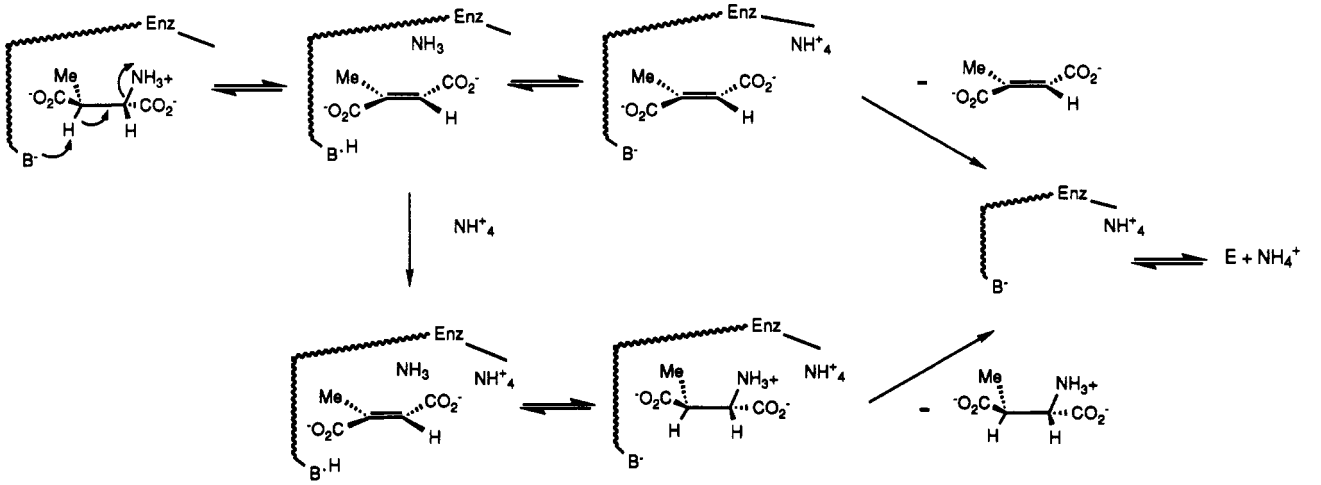

inhibition experiments were conducted at high [K^+] (Figure 7B in supplementary material).

At low [NH_4^+] (0–100 mM), the product appeared to behave as an uncompetitive inhibitor and intersect ($1/V^{app}$) replots against [NH_4^+] were nonlinear. At much higher [NH_4^+], the product acted as a noncompetitive inhibitor.

For uni-bi mechanisms, products are not expected to act as uncompetitive inhibitors. Hence, it appeared that ammonium ion was able to bind to enzyme–substrate, enzyme–intermediate, or enzyme–product complexes in yet a third mode, in addition to as a substrate and as an activator. If, for a moment, the overall effect of product inhibition is believed and accepted to be noncompetitive, the result would indicate that ammonium ion is the first product off in a compulsory order deamination mechanism. However, the result was clearly too complex to interpret reliably and it was, after all, necessary to determine the product release order at low [K^+], where isotope effects for the deamination and hydrogen exchange reactions could be observed.

In order to achieve this objective, two experimental approaches were pursued. First, a competitive inhibitor for ammonium ion which would not serve as an activator for the enzyme was sought. A dead-end competitive inhibitor for the second substrate on, in an ordered bi-uni mechanism, should be an uncompetitive inhibitor for the first substrate and, if the addition is random, a noncompetitive (or an apparently competitive) inhibitor for the other substrate (Fromm, 1975).

Methylammonium ion did not serve as an activator and is a competitive inhibitor (K_i = 150 mM) for (2*S*,3*S*)-3-methylaspartic acid in the deamination reaction (Figure 8 in supplementary material) and a competitive inhibitor (K_i = 350 mM) for ammonia in the amination reaction (Figure 9 in supplementary material). Thus a suitable inhibitor had been identified. Note that in the amination reaction direction with no potassium ion present, the initial rate versus [NH_4^+]^2 double-reciprocal plots are linear, indicating that the dissociation constants for the substrate and activator sites for NH_4^+ are similar, ~45–60 mM (Figure 10 in supplementary material). The abscissa intercepts for plots of initial rate versus $1/[NH_4^+]$ at 1 mM K^+ at pH 9.0 (Figure 11 in supplementary material) and at high [K^+] at pH 5.9 (Bright, 1965) were not altered by varying the concentration of mesaconic acid, indicating that the presence of one substrate does not modify the binding affinity of the enzyme for the other. Since methylamine acted as a linear competitive inhibitor for mesaconic acid, mesaconic acid and ammonium ion must bind/debind in a random manner (Fromm, 1975).

In the second approach to probe the relative rates of product release from the enzyme, [^{15}N]ammonia–trideuteriomesaconic acid double isotope exchange experiments were performed under conditions where solvent exchange with the C-3 hydrogen is facile. Incubations contained unlabeled (2*S*,3*S*)-3-methylaspartic acid, [*methyl*-$^2H_3$]mesaconic acid, [^{15}N]-ammonium ion, and the relevant cofactors at pH 9.0. The concentrations of the various components were arranged such that deamination would be slightly favored. Enzyme was added and aliquots of the reaction mixture were removed at t = 0 and at various times thereafter. The amino acid isotopomers were purified and derivatized (see Materials and Methods) and the isotope distributions were analyzed by SIR-GCMS. Peak areas for the molecular ions corresponding to the various isotopomers were calculated and normalized with respect to the internal standard and the results were plotted against time (Figure 3).

The ratios of the labeled and unlabeled species present during the course of the reaction indicated that the unlabeled ammonium ion derived from the substrate was not trapped by the labeled mesaconic acid and that the formation of ^{14}N-labeled trideuterio substrate (represented by molecular ion 295) was due to the back reaction only. This is the expected result for a random mechanism or for a compulsory order mechanism in which ammonium ion debinds first. However, no unlabeled mesaconic acid was trapped on the enzyme by the labeled ammonium ion (trace for molecular ion 293, Figure 3; also see Results section). As the labeled ammonium ion was present at one-fifth of K_{NH_4}, sufficient to cause a substantial back reaction and an increase in hydrogen exchange (Bright, 1964), the result indicates that mesaconic acid is released by the enzyme at a rate equal to the rate of ammonium ion release and that the debinding mode is random. Repeat experiments confirmed this result.

Thus, the earlier observation that [^{15}N]ammonia-induced C-3 hydrogen exchange was not accompanied by the incorporation of ^{15}N label into the substrate had been verified (Bright, 1964), and in the context of the now-established debinding order and size of isotope effects, it could be argued that the increase in the hydrogen exchange reaction caused by ammonia resulted from retarding the *actual* release of the products from the enzyme.

To summarize the facts, in the absence of added ammonium ion the ratio v_{ex}/v_{deam} is dependent upon pH (Table III). At pH 9.0, the value of v_{ex}/v_{deam} is 1.0. Although increasing the ammonium ion concentration increases v_{ex}/v_{deam}, an increase due to the back reaction can be excluded because added am-

monium ion is not incorporated into the substrate pool. Since in the absence of added ammonium ion the exchange rate is high, it is evident that a step which follows C–H bond cleavage is slow. On the basis of the observed isotope effect for exchange, it appears that this slow step occurs after C–N bond cleavage, as, if exchange occurred before C–N bond cleavage, the observed isotope effects would be sensitive to the ratio v_{ex}/v_{deam}, which they are not. The possibility of ammonium ion serving as a cationic activator for the exchange reaction can be ruled out by the finding that the ratio v_{ex}/v_{deam} is not affected by potassium ion (Bright, 1964).

In consideration of these findings, the most reasonable explanation is that there is a slow step which occurs after C–N bond cleavage and before the formation of the E·NH_4·Mes complex which causes the products to partition between recombination (to give methylaspartic acid) and formation of the E·NH_4·Mes complex where the product can escape. Therefore, in labeled water, solvent-derived hydrogen could exchange with the conjugate acid on the enzyme (which as base removes a proton from the substrate at C-3) to give labeled substrate. Since ammonium ion enhances the exchange reaction, it must prevent the formation of the E·NH_4·Mes complex. Ammonium ion could easily do this if the product site for ammonium ion is not occupied in the intermediate complex by the amino group of the substrate, as illustrated in Scheme VIII. Substantial support for this notion is offered by the observation of nonlinear uncompetitive ammonium ion product inhibition for the deamination of the substrate. The uncompetitive mode of inhibition is indicative of the introduction of an irreversible step into a mechanism, while the nonlinearity suggests that two molecules of ammonia or ammonium ion can bind to a single form of the enzyme.

The results of this study, therefore, define the order of substrate, product, and metal ion binding and demonstrate that binding order is pH dependent and that two catalytically active forms of the enzyme exist. The results also show that there is an isotope effect for the exchange reaction and rationalize why primary deuterium isotope effects for the elimination reaction were not detected previously. The results do not exclude the possibility that the enzyme operates via a carbanion mechanism but provide no support for the notion. Work which addresses the chemical mechanism of the elimination process catalyzed by the enzyme when (2*S*,3*S*)-3-methylaspartic acid and (2*S*)-aspartic acid are the substrates is underway.

ACKNOWLEDGMENTS

We thank Dr. N. R. Thomas for preparing [*methyl*-$^2H_3$]-mesaconic acid and Dr. G. J. Langley for performing the mass spectrometric analyses of the phenylthiohydantoin derivatives.

SUPPLEMENTARY MATERIAL AVAILABLE

Eleven figures showing mass spectra of the phenylthiohydantoin ester derivatives of (2*S*,3*S*)-3-methylaspartic acid and [*methyl*-$^2H_3$]-(2*S*,3*S*)-3-methylaspartic acid, the effect of the potassium ion concentration on the deamination of 3-methylaspartic acid and the magnitude of the primary deuterium kinetic isotope effect, the effect of pH on the binding of potassium ion, the effect of potassium concentration on magnesium cation binding, the effects of magnesium ion concentration on the deamination reaction at different pH values, the effects of ammonia and methylamine as inhibitors for the deamination reaction, inhibition of the amination reaction by methylamine with respect to ammonia, dependence of the amination of mesaconic acid on ammonium ion concentration in the presence and absence of potassium ion, and the effect of mesaconic acid (17 pages). Ordering information is given on any current masthead page.

REFERENCES

Akhtar, M., Cohen, M. A., & Gani, D. (1986) *J. Chem. Soc., Chem. Commun.*, 1290.

Akhtar, M., Botting, N. P., Cohen, M. A., & Gani, D. (1987) *Tetrahedron 43*, 5899.

Barker, H. A., Smyth, R. D., Wawszkiewicz, E. J., Lee, M. N., & Wilson, R. M. (1958) *Arch. Biochem. Biophys. 78*, 468.

Barker, H. A., Smyth, R. D., Wilson, R. M., & Weissbach, H. (1959) *J. Biol. Chem. 234*, 320.

Botting, N. P., & Gani, D. (1989) in *Molecular Recognition, Chemical and Biochemical Problems*, Royal Society of Chemistry, Cambridge, U.K.

Botting, N. P., Akhtar, M., Cohen, M. A., & Gani, D. (1987) *J. Chem. Soc., Chem. Commun.*, 1371.

Botting, N. P., Akhtar, M., Cohen, M. A., & Gani, D. (1988a) *Biochemistry 27*, 2953.

Botting, N. P., Cohen, M. A., Akhtar, M., & Gani, D. (1988b) *Biochemistry 27*, 2956.

Bright, H. J. (1965) *J. Biol. Chem. 240*, 1198.

Bright, H. J. (1967) *Biochemistry 6*, 1191.

Bright, H. J., & Silverman, R. (1964) *Biochim. Biophys. Acta 81*, 175.

Bright, H. J. (1964) *J. Biol. Chem. 239*, 2307.

Bright, H. J., Ingraham, L. L., & Lundin, R. E. (1964a) *Biochim. Biophys. Acta 81*, 576.

Bright, H. J., Ingraham, L. L., & Lundin, R. E. (1964b) *Biochemistry 3*, 1224.

Cleland, W. W. (1987) *Bioorg. Chem. 15*, 283.

Fields, G. A., & Bright, H. J. (1970) *Biochemistry 9*, 3801.

Fromm, H. J. (1975) *Initial Rate Enzyme Kinetics*, Springer-Verlag, Berlin.

Hanson, K. R., & Havir, E. A. (1972) *Enzymes (3rd Ed.) 7*, 75.

Hermes, J. D., Weiss, P. M., & Cleland, W. W. (1985) *Biochemistry 24*, 2959.

Hsiang, M. W., & Bright, H. J. (1967) *J. Biol. Chem. 242*, 3079.

Hsiang, M. W., & Bright, H. J. (1969) *Methods Enzymol. 13*, 347.

Kim, S. C., & Raushel, F. M. (1986) *Biochemistry 25*, 4744.

King, E. L., & Altman, C. (1956) *J. Phys. Chem. 60*, 1375.

Leatherbarrow, R. J. (1987) Enzfitter, A non-linear regression data analysis program (from the Chemistry Department, Imperial College of Science, Technology and Medicine, London SW7 2AY, U.K.) published and distributed by Biosoft, Cambridge CB2 1JP, U.K.

Nuiry, I. I., Hermes, J. D., Weiss, P. M., Chen, C., & Cook, P. F. (1984) *Biochemistry 23*, 5168.

Thomas, N. R. (1990) Ph.D. Dissertation, University of Southampton, U.K.

Ueda, S., Sato, K., & Shimizu, S. (1982) *J. Nutr. Sci. Vitaminol. 28*, 21.

Viola, R. E., & Cleland, W. W. (1982) *Method Enzymol. 87*, 353.

Williams, V. R., & Traynham, J. G. (1962) *Fed. Proc. 21*, 247.

Winkler, M. F., & Williams, V. R. (1967) *Biochim. Biophys. Acta 146*, 287.

Wu, W. T., & Williams, V. R. (1968) *J. Biol. Chem. 243*, 5644.